

# Analysis of Drying Kinetics of a Slurry Droplet in the Falling Rate Period of Spray Drying

Boris Golman and Wittaya Julklang

**Abstract**—The heat and mass transfer was investigated during the falling rate period of spray drying of a slurry droplet. The effect of the porosity of crust layer formed from primary particles during liquid evaporation was studied numerically using the developed mathematical model which takes into account the heat and mass transfer in the core and crust regions, the movement of the evaporation interface, and the external heat and mass transfer between the drying air and the droplet surface. It was confirmed that the heat transfer through the crust layer was more intense in the case of the dense droplet than the loose one due to the enhanced thermal conduction resulting in the higher average droplet temperature. The mass transfer was facilitated in the crust layer of loose droplet owing to the large pore space available for diffusion of water vapor from the evaporation interface to the outer droplet surface. The longer drying time is required for the droplet of high porosity to reach the final moisture content than that for the dense one due to the larger amount of water to be evaporated during the falling rate.

**Keywords**—Spray Drying, Slurry Droplet, Heat and Mass Transfer, Crust Layer Porosity, Mathematical Modeling.

## I. INTRODUCTION

NANOPARTICLES are currently used or being under investigation for use in many high-value products and materials, starting from cosmetics, catalysts, sports equipment to polishing media and nanoscale electrode materials of lithium-ion batteries [1]. However, high cohesion and self-agglomeration of nanoparticles makes their handling on industrial scale challenging. To overcome this difficulty, the spray drying technology was applied for preparation of agglomerates of nanoparticles of improved flowability [2]. Spray drying was also investigated for production of agglomerates of controlled porous structure to be utilized as high-value functional materials [3].

Spray drying is the process involving generation of droplets by atomizing feed slurry, drying of droplets in contact with hot gas and separation of dried particles from exhaust gas. The drying rate, the droplet morphology and porous structure are determined by the rates of heat, mass and momentum transfer between the droplet and the drying gas as well as the heat and mass transfer inside the partially dried droplets. The drying mechanism is defined by the process conditions, slurry composition and droplets flow paths in the dryer chamber [4].

The drying process of a slurry droplet can be divided into two periods according to the droplet morphology. The droplet

shrinks during the first drying period as liquid evaporates from the droplet outer surface at constant drying rate. The second drying period starts with formation of a solid crust layer around the wet core. The drying rate significantly decreases during the falling rate period due to the decline of heat and mass transfer rates in the growing crust layer as vapor generated at the evaporation surface diffuses through the crust porous space to the outer droplet surface and the heat supplied by the drying gas is transferred to the evaporation surface by conduction [5].

The mathematical model of spray drying of the slurry droplet in the falling rate period was developed and validated in our previous study [6]. The temperature and moisture concentration distributions inside the crust and wet core regions were simulated taking into account both internal and external mass and heat transfer resistances.

The objective of the present study is to analyze the effect of porosity of porous structure of the crust layer on the drying kinetics of the slurry droplet in the falling rate period of spray drying.

## II. THEORETICAL

The droplet is composed of the dry porous crust layer and the wet core during the second period of drying. The evaporation takes place in the droplet on the boundary that separates the dry crust and wet core regions. The evaporation surface recedes inside the droplet, the wet core shrinks and the crust layer grows as the drying proceeds. The outside droplet radius remains constant during this stage.

### A. Heat and Mass Transfer in Dry Crust Layer

The temperature distribution in the radial direction of the dry crust layer composed of pore spaces and the solid structure is described by (1). The crust layer is assumed to be of uniform porosity. The accumulation of thermal energy in the layer is balanced by the flow of energy by conduction through the layer. Here, the heat accumulation is neglected in pore spaces filled with air and water vapor.

$$\frac{\partial}{\partial t}((1-\varepsilon)\rho_s C_p T_{cr}) = \frac{1}{r^2} \frac{\partial}{\partial r} \left( k_{cr} r^2 \frac{\partial T_{cr}}{\partial r} \right) \quad (1)$$

where  $r$  is radial position in the crust layer,  $T_{cr}$  is the temperature,  $\varepsilon$  is the porosity of crust layer,  $k_{cr}$  is the effective heat conductivity of crust layer, and  $\rho_s$  and  $C_p$  are the density and the heat capacity of solid material,

B. Golman\* and W. Julklang are with the School of Chemical Engineering, Institute of Engineering, Suranaree University of Technology, Nakhon Ratchasima, 30000 Thailand (\*corresponding author, phone:+66-4422-4325; fax: +66-4422-4609; e-mail: golman@sut.ac.th).

respectively.

The vapor concentration in the crust layer is obtained from the mass balance (2). This equation was formulated assuming that the accumulation of water vapor in pore spaces balances the transfer of water vapor to the outer droplet surface by diffusion,

$$\frac{\partial}{\partial t}(\varepsilon C_{wv}) = \frac{1}{r^2} \frac{\partial}{\partial r} \left( D_{cr} r^2 \frac{\partial C_{wv}}{\partial r} \right) \quad (2)$$

where  $C_{wv}$  is the vapor concentration and  $D_{cr}$  is the effective diffusivity of crust layer.

### B. Heat Transfer in Wet Core

The temperature distribution in the wet core comprising of solid particles dispersed in the liquid phase is expressed as

$$\frac{\partial}{\partial t}(\varepsilon \rho_l C_{p_l} + (1-\varepsilon) \rho_s C_{p_s} T_{co}) = \frac{1}{r^2} \frac{\partial}{\partial r} \left( k_{co} r^2 \frac{\partial T_{co}}{\partial r} \right) \quad (3)$$

where  $k_{co}$  is the heat conductivity of wet core, and  $\rho_l$  and  $C_{p_l}$  are the density and heat capacity of liquid phase, respectively.

### C. Boundary Conditions

The heat balance on the evaporation interface separating the crust layer and the wet core is given as

$$\varepsilon \rho_l \lambda_l \frac{ds}{dt} = -k_{cr} \frac{\partial T_{cr}}{\partial r} + k_{co} \frac{\partial T_{co}}{\partial r} \quad (4)$$

where  $s$  is the radial position of the evaporation interface and  $\lambda_l$  is the latent heat of water evaporation.

Here we assume that heat delivered to the interface from the outer droplet surface by conduction through the crust layer is consumed for liquid evaporation and heating of the wet core by conduction to the core center.

The mass balance on the evaporation interface is

$$\varepsilon \rho_l \frac{\partial s}{\partial t} = D_{cr} M_l \frac{\partial C_{lv}}{\partial r} \quad (5)$$

where  $M_l$  is the molecular weight of water.

The heat and mass balances on the outer droplet surface,  $R_m$  are

$$-k_{cr} \frac{\partial T_{cr}}{\partial r} \Big|_{r=R_m} = k_h (T_{cr}(R_m) - T_{gas}) \quad (6)$$

$$-D_{cr} \frac{\partial C_{lv}}{\partial r} \Big|_{r=R_m} = k_m (C_{lv}(R_m) - C_{gas}) \quad (7)$$

where  $k_h$  and  $k_m$  are the convective heat and mass transfer coefficients, and  $T_{gas}$  and  $C_{gas}$  are the temperature and vapor concentration in the bulk gas phase, respectively.

The variation of droplet weight with drying time is calculated as a function of position of evaporation interface  $s$ ,

$$W_d = \frac{4}{3} \pi [\rho_w \varepsilon s^3 + \rho_s (1-\varepsilon) R_m^3] \quad (8)$$

The average droplet temperature is evaluated by integration of temperature distributions in the crust layer and wet core

$$T_{av} = \frac{3}{R_m^3} \int_0^{R_m} r^2 T(r) dr \quad (9)$$

### D. Crust Layer Structural Relationships

The effective heat conductivity of crust layer is estimated using Woodside and Messmer [7] model. A model (10) was derived by combining contributions of the series and parallel distributions of solid and fluid phases in the porous structure relative to the direction of heat flow [8].

$$k_{cr} = \frac{a \cdot k_s \cdot k_f}{k_s \cdot (1-d) + d \cdot k_f} + c \cdot k_f \quad (10)$$

where  $c = \varepsilon - 0.03$ ,  $a = 1 - c$  and  $d = (1 - \varepsilon) / a$ . Here,  $k_f$  and  $k_s$  are the heat conductivities of fluid and solid phases, respectively.

Using Archie's [9] empirical equation, the effective diffusivity is evaluated as

$$D_{cr} = D_{wv} \cdot \varepsilon^m \quad (11)$$

where the exponent  $m$  varied between 1.8 and 2.0. The value of  $m$  was set at 1.9 in our simulation.

The diffusivity of water vapor in air,  $D_{wv}$  is a function of temperature [10];

$$D_{wv} = 0.220 \times 10^{-4} (T / 273.15)^{1.75} \quad (12)$$

The convective heat and mass transfer coefficients are evaluated from Ranz and Marshall correlations [11] as

$$Nu = \frac{h(2R_m)}{k_g} = 2 + 0.65 Re^{0.5} Pr^{0.33} \quad (13)$$

$$Sh = \frac{k_m(2R_m)}{D_{wv}} = 2 + 0.65 Re^{0.5} Sc^{0.33} \quad (14)$$

where  $Nu$ ,  $Sh$ ,  $Re$ ,  $Pr$  and  $Sc$  are the Nusselt, Sherwood, Reynolds, Prandtl and Schmidt numbers for drying air, respectively. These dimensionless numbers are defined as

$$Re = \frac{2R_{in}v_g\rho_g}{\mu_g}, Pr = \frac{Cp_g\mu_g}{k_g}, Sc = \frac{\mu_g}{\rho_g D_{wv}} \quad (15)$$

where  $v_g$  is the gas velocity, and  $Cp_g$ ,  $k_g$ ,  $\rho_g$  and  $\mu_g$  are the heat capacity, the heat conductivity, the density and the viscosity of drying air, respectively.

The system of partial and ordinary differential equations with moving boundary was solved numerically by a finite difference method using an implicit scheme [10], [12].

### III. RESULTS AND DISCUSSION

The spray drying of the slurry droplet of nanosized silica particles was investigated at the constant temperature of 200°C and velocity of 1.0m/s of the drying air. The droplet radius was kept fixed at 25µm during the falling rate period. The crust layers of different porosities, 0.40, 0.45 and 0.50, were used to study the effect of layer porous structure on the drying kinetics of slurry droplet.

The decrease of droplet weight with drying time is illustrated in Fig. 1 for droplets of various porosities. The weight was normalized by the droplet weight at the beginning of the falling rate period and the starting point of the drying time calculation also defaults to the beginning of this period. The size and final moisture content are chosen to be the same for droplets of various porosities as they are usually specified by the process requirements.

Assuming that the final moisture content of the droplet is  $m_f$ , the amount of water left in the droplet after drying,  $w_f$ , is defined as

$$w_f = \frac{\rho_s(1-\varepsilon)\left(\frac{4}{3}\pi R_{in}^3\right)}{1-m_f} \quad (16)$$

The loose droplet of high porosity contains large amount of water at the beginning of the falling rate period when water fills all spaces in the droplet not occupied by solid. At the same time, according to (16), the amount of water in the loose droplet is low at the end of drying to satisfy the final moisture content. As a result, the longer time is required for drying the loose droplet in comparison with the dense one as the larger amount of water to be evaporated from the loose droplet during the falling rate period.

The drying rate decreases with the progress of drying owing to the decline in the rates of heat transfer from the droplet outer surface to the evaporation interface and the mass transfer of water vapor in opposite direction as a result of the growing crust layer, as shown in Fig. 2.

The thicker crust layer is formed in the dense droplet than in the loose one for the same drying time. This can be

attributed to the enhanced rate of heat transfer by conduction in the crust layer as confirmed by the higher value of effective heat conductivity by (10), as illustrated in Fig. 3.

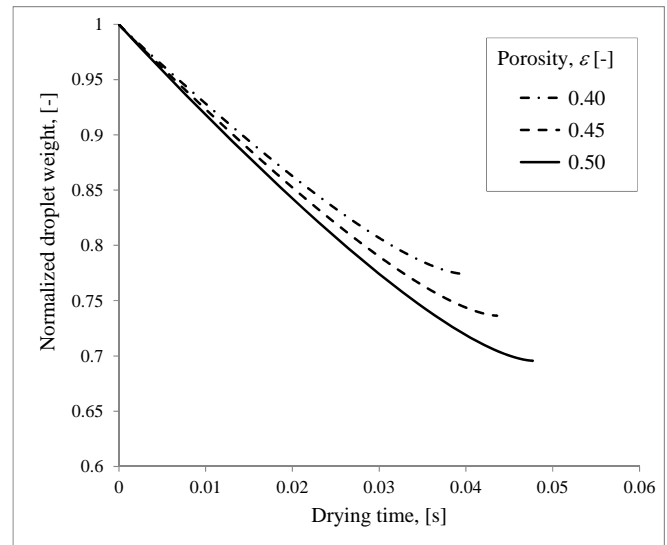


Fig. 1 Variation of droplet weight with drying time

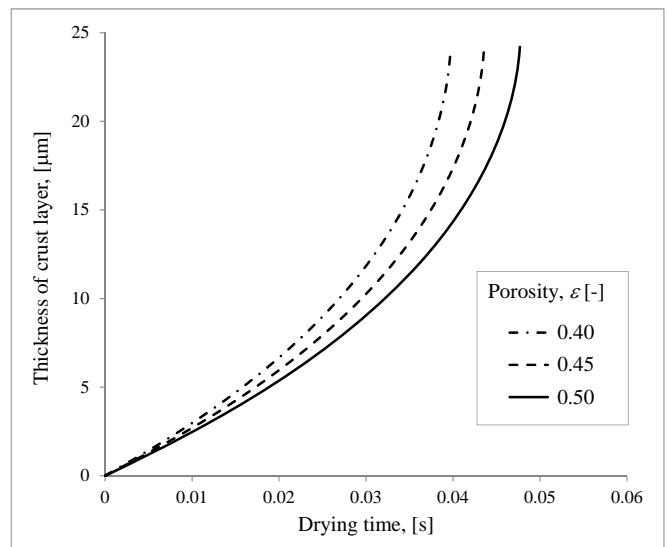


Fig. 2 Thickness of crust layer as function of drying time

The increase of droplet average temperature with drying time is shown in Fig. 4. The average temperature of dense droplet is higher than that of loose one due to the higher effective heat conductivity of thicker crust layer which can be ascribed to the larger amount of solid phase of high conductivity.

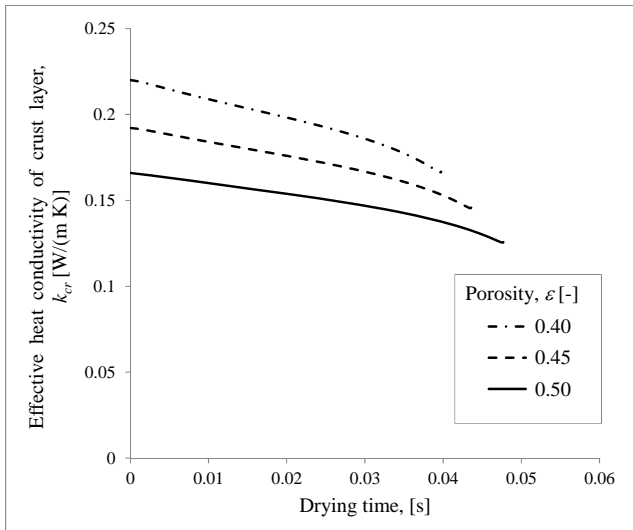


Fig. 3 Variation of effective conductivity of crust layers of various porosities with drying time

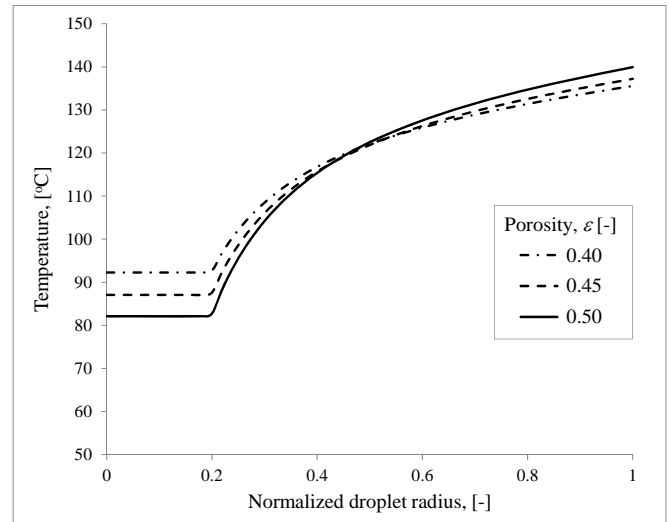


Fig. 5 Temperature distribution in the droplet

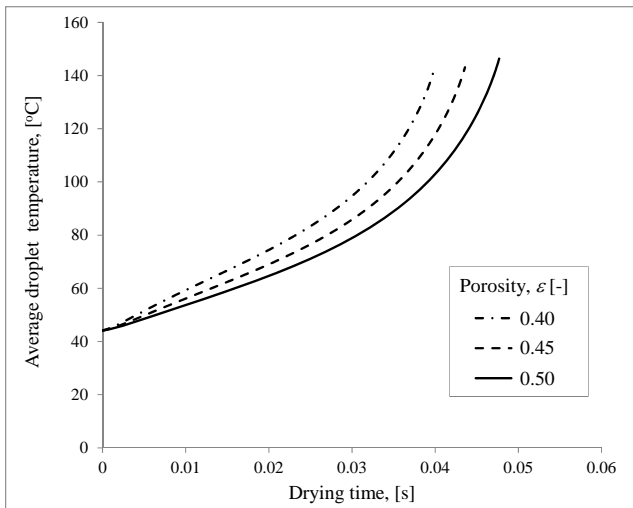


Fig. 4 Variation of droplet average temperature with drying time

The temperature distributions in the radial direction of droplets of various porosities are illustrated in Fig. 5. These profiles were evaluated at different drying times corresponding to the same position of evaporation interface. The temperature of core region only slightly increases in the radial inward direction. However, there is a significant temperature gradient in the crust region due to the heat transfer resistance of porous layer. The heat supply to the core-crust interface of high porosity droplet is limited by the low effective heat conductivity of crust layer resulting in the low temperature at the evaporation interface.

The distributions of water vapor concentration in the radial direction of crust layer are illustrated in Fig. 6 for droplets of various porosities. The vapor concentration is lower in the crust region of the loose droplet in comparison with the dense one as less vapor produces at the evaporation interface of loose droplet due to the low interface temperature. The generated water vapor quickly diffuses to the outer droplet surface through the large pore spaces of the high porosity droplet. This is confirmed by the enhanced value of effective diffusivity in Fig. 7, in spite of the slightly lower coefficient of molecular diffusion at low temperature by (12).

The effective diffusivity of water vapor in the porous space of crust layer increases with drying time as the temperature rises in the layer by (11), as illustrated in Figs. 4 and 7.

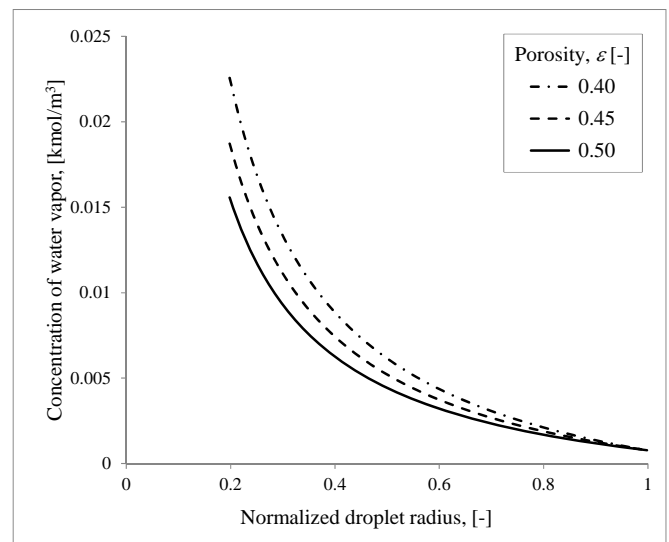


Fig. 6 Distribution of concentration of water vapor in the crust layer

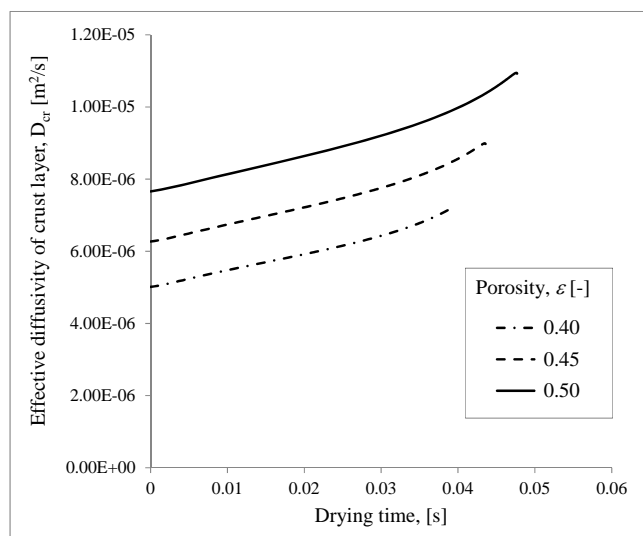


Fig. 7 Variation of effective diffusivity of crust layers of various porosities with drying time

#### IV. CONCLUSION

The kinetics of spray drying of the slurry droplet was studied in the falling rate period using the comprehensive mathematical model that takes into account the heat and mass balances in the crust layer and wet core region. The effect of the porous structure of crust layer was investigated on the drying kinetics by changing the layer porosity.

As a result, the longer drying time was required in the case of the loose droplet during the falling-rate period as the large amount of water to be evaporated to attain the same final moisture content as the dense droplet of identical size.

The average temperature of dense droplet was higher than that of loose one due to the higher value of effective conductivity of crust layer of dense droplet.

The heat transfer through the crust layer by conduction was more profound in the case of the dense layer owing to the high amount of solid phase of high conductivity. However, the mass transfer was accelerated in the crust layer of the loose droplet because of the large pore spaces available for diffusion of water vapor.

The present analysis can be extended to include the description of formation of porous crust layer which will be useful for optimization of process parameters with the aim of production of particles of desired porous structure.

#### ACKNOWLEDGMENT

The authors would like to thank the National Research Council of Thailand for their funding of this research.

#### REFERENCES

- [1] B. Bhushan, Ed., *Springer Handbook of Nanotechnology*, 3rd ed. New York: Springer, 2010.
- [2] K. Sollohub, and K. Cal, "Spray drying technique: II. Current applications in pharmaceutical technology," *Journal of Pharmaceutical Sciences*, Vol. 99, pp. 587–597, 2010.
- [3] A. B. Nandiyanto, and K. Okuyama, "Progress in developing spray-drying methods for the production of controlled morphology particles:

From the nanometer to submicrometer size ranges," *Advanced Powder Technol.*, vol. 22, pp. 1–19, 2011.

- [4] K. Masters, *Spray Drying Handbook*, Longman Scientific and Technical, Harlow, England, 1985.
- [5] M. Mezhericher, A. Levy, and I. Borde, "Theoretical models of single droplet drying kinetics: a review", *Drying Technology*, Vol. 28, pp. 278–293, 2010.
- [6] W. Julklang, and B. Golman, "Influence of operational conditions on the drying kinetics of a slurry droplet in a spray dryer," *Engineering Transactions*, Vol. 15, pp. 59–65, 2012.
- [7] W. Woodside, and J.H. Messmer, "Thermal conductivity of porous media. I. Unconsolidated sands," *J. Appl. Phys.*, vol. 32, 1688, 1961.
- [8] I.H. Tavman, "Effective thermal conductivity of granular porous materials," *Int. Comm. Heat Mass Transfer*, vol. 23, pp. 169–176, 1996.
- [9] G. E. Archie, "The electrical resistivity log as an aid in determining some reservoir characteristics," *Trans. AIME*, vol. 46, pp. 45–61, 1942.
- [10] N. Dalmaz, H.O. Ozbelge, A.N. Eraslan, and Y. Uludag, "Heat and mass transfer mechanisms in drying of a suspension droplet: a new computational model", *Drying Technology*, Vol. 25, pp. 391–400, 2007.
- [11] W.E. Ranz, and W.R. Marshall, "Evaporation from drops", *Chemical Engineering Progress*, vol. 48, pp. 141–146, 1952.
- [12] J. Crank, *Free and Moving Boundary Problems*, Clarendon Press, Oxford, 1984.